Influence of the Fine Structure on the Response of Polymer Chains to Perturbation Fields

Gustavo Dominguez-Espinosa,[†] Ricardo Díaz-Calleja,[†] Evaristo Riande,*[,‡] Ligia Gargallo,[§] and Deodato Radic[§]

Departamento de Termodinámica Aplicada, ETSII, Universidad Politécnica de Valencia, Valencia, Spain; Instituto de Ciencia y Tecnología de Polímeros (CSIC), 28006 Madrid, Spain; and Departamento de Química Física, Pontificia Universidad Católica de Chile, Santiago, Chile

Received November 8, 2005; Revised Manuscript Received February 6, 2006

ABSTRACT: The relaxation behavior of poly(3-methylbenzyl methacrylate), poly(3-fluorobenzyl methacrylate), and poly(3-chlorobenzyl methacrylate) was thoroughly studied by broadband dielectric spectroscopy with the aim of investigating the influence of slight differences in chemical structure on the response of polymers to electric perturbation fields. Retardation spectra calculated from dielectric isotherms utilizing linear programming regularization parameter techniques were used to facilitate the deconvolution of strongly overlapped absorptions. Above the glass transition temperature, the spectra of the two halogenated polymers present a secondary γ process well separated from a prominent peak resulting from the overlapping of the α and β relaxations. The spectra of poly(3-methylbenzyl methacrylate) exhibit at long times a well-developed α absorption followed in decreasing order of time by two weak absorptions, named β and γ, whose intensities increase with temperature. The temperature dependence of the distance of the α peak from the β and γ peaks, expressed in terms of $\log(f_{\max,\beta}/f_{\max,\alpha})$ and $\log(f_{\max,\gamma}/f_{\max,\alpha})$, respectively, is studied. The Williams ansatz and the extended ansatz give a fairly good account of the relaxation behavior of the polymers. The stretch exponent associated with the α relaxation increases with temperature from ca. 0.2 at low temperatures to the vicinity of 0.5 at high temperatures. At low temperatures, the α relaxation is described by a Vogel-type equation, but at high temperature the β and α processes are roughly described by the same Arrhenius equation. In the whole temperature range, the activation energy o the γ relaxation is significantly lower than that of the β absorption. The mechanisms involved in the development of the secondary relaxations are qualitatively discussed.

Introduction

During the cooling process, supercooled liquids may reach a temperature at which the single dielectric absorption they exhibit in the moderate supercooled regime splits into a slow α relaxation arising from cooperative molecular motions and a fast β relaxation produced by restricted motions in a variety of local environments.[1,2] The temperature, T_x, at which the splitting occurs is believed to be related to the onset of cooperativity of the α relaxation[3] and to the critical temperature, T_c,[4] of the model coupling theory.[5,6] In fact, the information at hand suggests that the ratio T_x/T_g for fragile glass-formers lies in the range 1.20−1.35.[7] Cooling the system further, a temperature is reached in the vicinity of which the α relaxation becomes frozen, ergodicity is lost, and the transition supercooled liquid−glass occurs.[8] Therefore, the dynamic α relaxation is a precursor of both the glassy state and the viscous flow.

A long time ago, Williams[9,10] discovered the merging of the β and α processes for poly(ethyl methacrylate) (PEM) to form the combined $\alpha\beta$ process through the use of applied pressure. Further work showed that the merging of the α and β relaxations depends on the chemical structure.[11−20] For example, a strong β relaxation in syndiotactic poly(methyl methacrylate) (PMM) dominates the dielectric losses,[15] a behavior not shared by the rest of poly(*n*-alkyl methacrylate)s. The effect of the increase of the length of the alkyl residue on the relaxation behavior of poly(*n*-alkyl methacrylate)s was studied in a systematic way by Donth and co-workers,[3,16,17] finding that the α relaxation of PEM coexists with the β process in the low-temperature region. The α process eventually vanishes at temperatures not far above T_g. At higher temperature, the β process of PEM acts as a precursor of a second α relaxation whose temperature dependence is also described by the Vogel−Fulcher−Tamman−Hesse equation,[21] but the fitting parameters differ from those found for the low-temperature α process.[17] A dramatic change in the splitting behavior of poly(*n*-butyl methacrylate) (PBM) happens.[3] In this polymer, contrary to what occurs in PEM, a unique α relaxation covers a wide range of temperature which further vanishes at high temperature. The Arrhenius plot of the α relaxation of PBM becomes parallel to that of the β absorption at high temperature, suggesting a mutual dependence of these two processes in the splitting region. More recent work carried out on poly(5-acryloxymethyl-5-methyl-1,3-dioxacyclohexane) (PMMD) shows that the mechanisms associated with the β relaxation have the same activation energy in the glassy state, the rubbery state, and the splitting region.[20] The α relaxation of PMMD vanishes in the vicinity of the splitting temperature while the strength of the β process experiences a rather sharp increase at $T > T_x$. A different scenario presents poly(2,3-dichlorobenzyl methacrylate) (PDCBM) where the β relaxation exhibits a crossover temperature, T_{co}, below which the activation energy associated with this process is significantly larger than above T_{co}. Moreover, the α and β relaxations maintain the same temperature dependence at $T > T_{co}$, suggesting a strong interdependence of these two processes in the splitting region.[22]

These previous observations prompted us to investigate how minor changes in the chemical structure may affect the splitting behavior of poly(methacrylate)s containing phenyl groups in the alcohol residue. For this purpose we have measured the

[†] Universidad Politécnica de Valencia.
[‡] Instituto de Ciencia y Tecnología de Polímeros (CSIC).
[§] Pontificia Universidad Católica de Chile.

10.1021/ma052381c CCC: $33.50
Published on Web 03/07/2006

Scheme 1. Schematic Representation of the Repeating Unit of Poly(3-methylbenzyl methacrylate) (R = CH_3), Poly(3-fluorobenzyl methacrylate) (R = F), and Poly(3-chlorobenzyl methacrylate) (R = Cl)

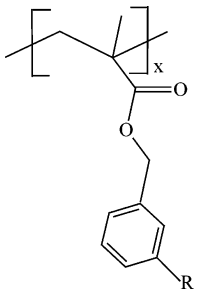

dielectric relaxation behavior of the polymers resulting from replacing the hydrogen atom in position 3 of the phenyl group of poly(benzyl methacrylate) by a methyl group, a chlorine atom, and a fluorine atom. In short, this work reports the relaxation behavior of poly(3-methylbenzyl methacrylate) (P3MM), poly-(3-chlorolbenzyl methacrylate) (P3CM), and poly(3-fluorobenzyl methacrylate) (P3FM) as studied by broadband dielectric spectroscopy. The repeating units of these polymers are given in Scheme 1. Taking into account that a Debye-type relaxation, being a single-exponential decay function in time domain, corresponds to a Dirac delta function in the retardation time spectra, the α and β relaxations overlapping in the frequency domain were resolved using the retardation spectra calculated from the dielectric loss isotherms. Special attention is paid to the contribution of the different relaxations to the total decay relaxation function.

Experimental Part

3-Methylbenzyl methacrylate, 3-chlorobenzyl methacrylate, and 3-fluorobenzyl methacrylate were obtained respectively by reaction of methacryloyl chloride with 3-methylphenylmethanol, 3-chlorophenylmethanol, and 3-fluorophenylmethanol, at room temperature. Polymerization of the respective monomers was carried out via a free radical process in toluene solution under a nitrogen atmosphere, at 323 K, using azobis(isobutyronitrile) as initiator. The polymers were precipitated with methanol, dissolved in chloroform, precipitated again with methanol, and finally dried at 60 °C in a vacuum oven. The weight-average molecular weights of the polymers determined by GPC were 130 000, 145 000, and 230 000 for P3MM, P3CM, and P3FM, respectively, the heterodispersity molecular weight index lying in the vicinity of 2. The stereochemical structure of poly(benzyl methacrylate)s obtained by free radical polymerization is atactic.

The glass transition temperature, T_g, of each polymer was determined with a TA DSC-Q10 apparatus at a constant heating rate of 20 K/min, under a nitrogen atmosphere. Each sample was heated twice, and the middle point of the endothermic step during the second scan was taken as the glass transition temperature. The values of T_g for P3MM, P3CM, and P3FM were respectively 307, 296, and 319 K.

Thermally stimulated depolarizaton current (TSDC) curves were obtained on polarized sample molded disks of 0.2 mm thickness and 10 mm of diameter, using a TSC/RMA TherMold 9000 apparatus. The global temperature dependence of the discharge intensity current was obtained by poling the pills under an electric potential of 350 V/mm, 10 K above T_g, for 3 min and further quenching at 113 K. Then the electric field was removed, and the poled samples were short-circuited for 1 min to remove free charges. Thermally stimulated depolarization curves were obtained by warming the electrode assembly at a constant heating rate of 7 K/min. From the time derivative of the polarization, the global discharge current curve as a function of temperature was obtained. Partial polarization discharge curves were also obtained in the glassy state, using poling windows of 5 K.

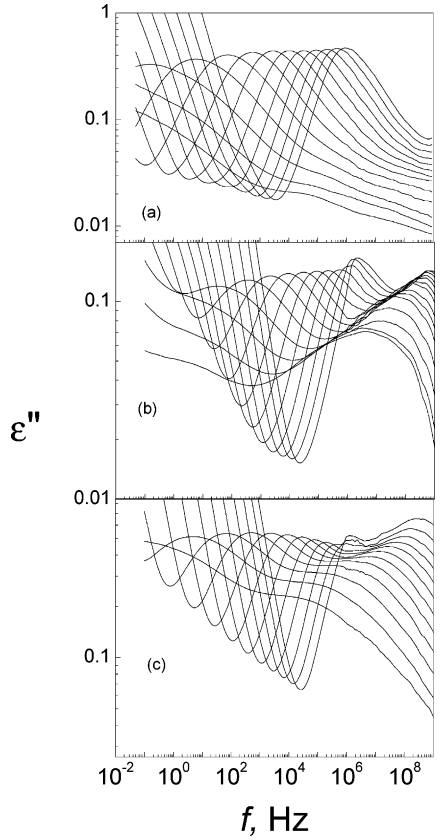

Figure 1. Dielectric loss in the frequency domain for poly(3-methylbenzyl methacrylate) (top), poly(3-fluorobenzyl methacrylate) (middle), and poly(3-chlorobenzyl methacrylate) in the temperature ranges 283−403, 293−423, and 293−403 K, respectively, at 10 K steps.

Complex dielectric permittivity measurements were performed over the frequency window $10^{-1}-10^{9}$ Hz, using a Novocontrol broadband dielectric spectrometer (Hundsangen, Germany) integrated by a SR 830 lock-in amplifier with an Alpha dielectric interface and an Agilent 4991 coaxial line reflectometer to carry out measurements in the frequency ranges $10^{-1}-10^{6}$ and $1 \times 10^{6}-1 \times 10^{9}$ Hz, respectively. In the latter case, the complex permittivity was determined by measuring the reflection coefficient at a particular reference plane. The temperature was controlled by nitrogen jet (QUATRO from Novocontrol) with a temperature error of ≈0.1 K during every single sweep in frequency. Isothermal measurements were carried out on molded disk-shaped samples of about 0.1 mm thickness, with diameters of 20 and 10 mm for frequencies lower and higher than 10^{6} Hz, respectively. Glass fiber spacers were used to ensure the stability of the sample thickness at high temperatures.

Results

Isotherms representing the dielectric loss in the frequency domain for P3MM, P3CM, and P3FM are shown at several temperatures in Figure 1. At first sight, significant differences are observed in the isotherms of the three polymers, despite the small variation of their respective chemical structures. The loss curves for P3MM display a well-developed α relaxation at temperatures slightly above the glass transition temperature followed in increasing order of frequency by two apparently weak secondary processes, named β and γ.

At difference of P3MM, the loss curves for P3CM and P3FM present a prominent secondary relaxation well separated from the dynamic α relaxation in the whole temperature range in such a way that the single αβ absorption displayed by the relaxation spectra of most systems[3,14−20,22] is not detected in these polymers. The apparent absence of the αβ absorption led us to

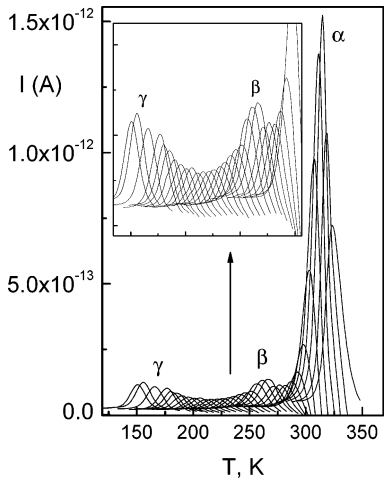

Figure 2. Partial thermally stimulated depolarization currents of P3FM at polarization temperatures from 133 K (first curve on the left side) to 318 K (last curve on the right side), 5K step. In the inset, details of the low-temperature depolarization curves are shown.

investigate the relaxations displayed by these polymers using depolarization current techniques. The global thermally stimulated depolarization current intensity curve for P3FM presents the γ absorption at short times followed by a prominent α peak which exhibits a small shoulder in the low-temperature region corresponding to the β process. The three absorptions are also displayed in the partial thermally stimulated depolarization curves represented in Figure 2.

Dielectric Retardation Spectra. Since the relaxation response of polymers to perturbation fields is more clearly defined in the retardation time spectra than in the loss curves in the frequency domain, we proceeded to determine the dielectric retardation spectra of the polymers as briefly indicated below. According to the linear phenomenology of dielectrics, the dielectric loss can be written as[9,11]

$$\epsilon''(\omega) = \left(\frac{\sigma}{\epsilon_0 \omega}\right)^S + \int_{-\infty}^{\infty} L(\ln \tau) \frac{\omega\tau}{1+\omega^2\tau^2} \, \mathrm{d} \ln \tau \qquad (1)$$

where L is the retardation spectrum, σ is the conductivity, and ϵ_0 is the permittivity in a vacuum while s accounts for the departure of the conductivity contribution from pure ionic conductivity ($s = 1$) as a consequence of interfacial blocking electrodes effects and other phenomena. Equation 1 can be written in an approximate way as[20,22]

$$\frac{\epsilon''(\omega_i)}{\rho_i} \cong \left(\left(\frac{\sigma}{\epsilon_0 \omega_i}\right)^s + \sum_{k=1}^{m} R_{ik} L(\ln \tau_k)\right)/\rho_i \qquad (2)$$

where

$$R_{ik} = \frac{\omega_i \tau_k}{1+\omega_i {\tau_k}^2} \ln\left(\frac{\tau_{k+1}}{\tau_{k-1}}\right)^{1/2}$$

The parameter ρ_i denotes the absolute experimental error involved in the determination of the dielectric loss $\epsilon''(\omega_i)$, and ω_i ($i = 1, 2, 3, ..., n$) represents the angular frequencies at which the experimental values of the dielectric loss were obtained. The conductivity contribution is not a limitation for the calculation of the retardation spectrum because it is an independent term in eq 2. We can write eq 2 in matricial form as

$$\begin{bmatrix} \frac{\epsilon''(\omega_1)}{\rho_1} \\ ... \\ ... \\ \frac{\epsilon''(\omega_n)}{\rho_n} \end{bmatrix} = \left\{ \begin{bmatrix} R_{11}...R_{1(m)} \\ .... \\ .... \\ R_{n1}...R_{n(m)} \end{bmatrix} \begin{bmatrix} L_1(\ln \tau_1) \\ ... \\ ... \\ ... \\ ... \\ L_{(m)}(\ln \tau_m) \end{bmatrix} + \left(\frac{\sigma}{\epsilon_0}\right)^s \begin{bmatrix} {\omega_1}^{-s} \\ .... \\ .... \\ {\omega_n}^{-s} \end{bmatrix} \right\} \begin{bmatrix} \frac{1}{\rho_1} \\ ... \\ ... \\ ... \\ \frac{1}{\rho_n} \end{bmatrix} \qquad (3)$$

where an equal log spaced retardation time vector with (m) elements is used. Equation 3 represents an indeterminate system of n equations and $m + 2$ incognita ($m > n$). The numeric treatment for the solution of the ill-conditioned eq 3 is similar to that of the also-ill posed quadratic programming minimization of[23]

$$\sum_{i=1}^{n} \left| \frac{\epsilon''(\omega_i)}{\rho_i} - \left(\sum_{k=1}^{m} R_{ik} L_k + \left(\frac{\sigma}{\epsilon_0 \omega_i}\right)^s\right) \frac{1}{\rho_i} \right|^2 + \lambda [\mathbf{L}^{\mathrm{T}}][\mathbf{H}][\mathbf{L}]$$

varying the retardation times vector (**L**), the ionic conductivity (σ), and the exponent s. Notice that this expression consists of two positive parts: the first accounts for the difference between experimental data and the calculated spectrum, and the second is a weighted term that accounts for the constriction of the smoothness of the retardation time spectra. Moreover, λ (>0) is a regularization parameter, and **H** is a definite positive quadratic form, the election of which must be based on the a priori knowledge of the solution. If the solution is thought to be piecewise linear, a good choice is $\mathbf{H} = \mathbf{B}^{\mathrm{T}}\mathbf{B}$, where **B** is the $(m - 2) \times m$ matrix[23]

$$\mathbf{B} = \begin{bmatrix} -1 & 2 & -1 & 0 & 0 & ... & 0 \\ 0 & -1 & 2 & -1 & 0 & ... & 0 \\ .... & & & & & & \\ 0 & ..... & -1 & 2 & -1 & 0 & \\ 0 & ..... & 0 & -1 & 2 & -1 & \end{bmatrix} \qquad (4)$$

and $\mathbf{B}^{\mathrm{T}}$ reads for the transpose of the matrix **B**. The solutions corresponding to different values of the regularization parameter λ were obtained by means of an iterative technique (conjugated gradient) that allows the utilization of the projection onto convex sets (POCS) methods for achieving a nonnegative solution, and the suitable λ parameter was determined in each case by means of the Morozov discrepancy method.[24] Since the intensity of Debye relaxations falls to the 1% of its maximum value for $\omega\tau = 10^{\pm 2}$, it is expected that the spectrum calculated from values of τ lying 2 decades above and below the reciprocal of the two extreme values of the frequency does not involve serious errors. This method differs from others based on the spectra formalism, such as the CONTIN program[25] (see, for example, ref 42 in ref 25), in the way of dealing with the conductivity contribution, the determination of a nonaliased solution, the method utilized to determine the regularization parameter, and the computational efficiency of the general methods for solving quadratic programming problems.

To investigate how truncation loss data, through frequency band limitation, may affect the range over which reliable $L(\ln \tau)$ values can be determined, truncations were performed on the loss curves and the spectra calculated. Illustrative plots showing the spectra calculated from truncations carried out at low frequencies in the isotherm at 323 K of P3FM are shown in Figure 3. It can be seen that the spectra at long times are rather independent of the truncation points provided that they are performed at $\omega < \omega_{\max}$, where $\omega_{\max}$ is the frequency associated with the maximum of the α relaxation. The same

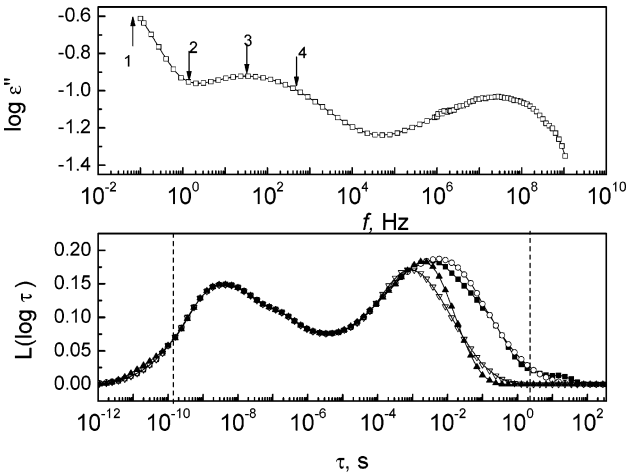

Figure 3. Illustrative plots showing how truncations in the dielectric loss isotherm of poly(3-fluorobenzyl methacrylate) at 323 K may affect the retardation spectra. Full square, open circles, full triangle, and open triangles correspond to truncation at 1, 2, 3, and 4, respectively. Values of $L(\log \tau)$ at high and low frequencies out of the limits indicated by vertical dash lines should be regarded as approximate.

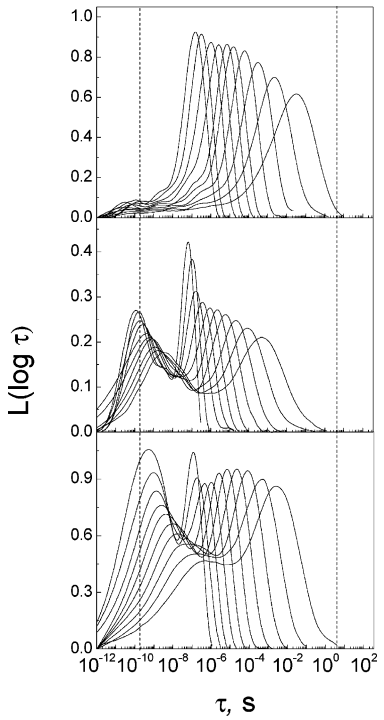

Figure 4. Retardation spectra for poly(3-methylbenzyl methacrylate) (top), poly(3-fluorobenzyl methacrylate) (middle), and poly(3-chlorobenzyl methacrylate) in the temperature ranges 313−403, 333−423, and 313−403 K, respectively, at 10 K steps. Values of $L(\log \tau)$ at high and low frequencies out of the limits indicated by vertical dash lines should be regarded as approximate.

occurs with the spectra at short times if the truncations are performed at $\omega > \omega_{max}$, where ω_{max} is the frequency associated with the maximum of the γ relaxation. In any case, the ranges over which the retardation spectra curves have been determined experimentally are indicated by vertical dash lines in the pertinent figures.

The retardation spectra calculated for P3MM, P3CM, and P3FM are shown in Figure 4. The spectra of both P3CM and P3FM present an apparent α relaxation well separated from a secondary absorption. However, the fact that that the merging of both relaxations into a single absorption is not detected at high temperatures, and taking into account that an inspection

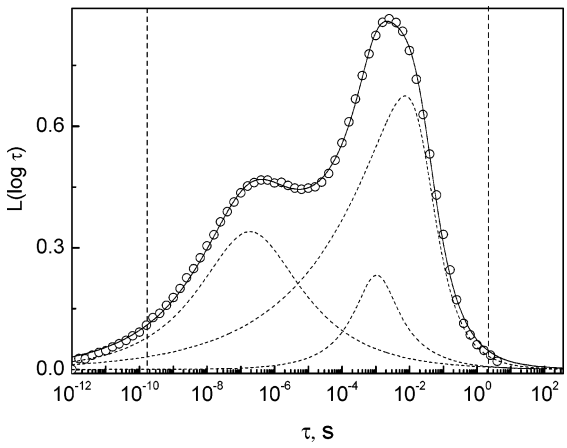

Figure 5. Deconvolution of the retardation spectrum for poly(3-chlorobenzyl methacrylate) at 313 K. Circles are experimental points while the continuous line represents the sum of the contributions of the α, β, and γ processes. Values of $L(\log \tau)$ at high and low frequencies out of the limits indicated by vertical dash lines should be regarded as approximate.

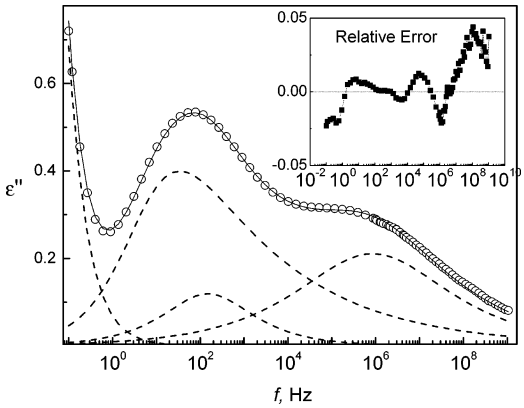

Figure 6. Comparison of the calculated dielectric loss from the spectrum (continuous curve) and the experimental results (circles) at 313 K for P3CM. The relative error of the calculations is shown in the inset. Contributions of the α, β, and γ processes are indicated by discontinuous curves.

of the current thermodepolarization curves suggests the presence of three absorption peaks, led us to investigate in detail the α absorption in the frequency domain of these two polymers.

The dipolar α relaxation is described by the Havriliak−Negami (H−N) equation[26]

$$\epsilon^*(\omega) = \epsilon_u + \frac{\epsilon_r - \epsilon_u}{[1 + (i\omega\tau_{HN})^a]^b} \quad (5)$$

where a and b are the H−N shape parameters, the subscripts r and u refer respectively to the relaxed and unrelaxed dielectric permittivity, and τ_{HN} is a characteristic retardation time. The inverse of this expression is the retardation spectrum associated with the α expression given by[27]

$$L_\alpha(\ln \tau) = \frac{1}{\pi} \frac{(\tau/\tau_{HN})^{ab} \sin b\theta}{[(\tau/\tau_{HN})^{2a} + 2(\tau/\tau_{HN})^a \cos a\pi + 1]^{b/2}} \quad (6)$$

where the parameter θ in eq 6 can be written as

$$\theta = \arctan\left(\frac{\sin \pi a}{(\tau/\tau_{HN})^a + \cos \pi a}\right) \quad (7)$$

if the argument of arctan is positive. If it is negative, then

$$\theta = \arctan\left(\frac{\sin \pi a}{(\tau/\tau_{HN})^a + \cos \pi a}\right) + \pi \tag{8}$$

On the other hand, since secondary relaxations are nearly symmetric, they can be described by the Fuoss−Kirkwood equation given by[28]

$$\epsilon''(\omega) = \frac{2\epsilon''_{max}(\omega/\omega_{max})^m}{1 + (\omega/\omega_{max})^{2m}} \tag{9}$$

where m accounts for the width of the distribution of retardation times and ϵ''_{max} is the dielectric permittivity at the peak maximum. The analytical expression for the retardation spectrum obtained from this expression is[29]

$$L_\beta(\ln \tau) = \frac{1}{\pi}\frac{2\cosh\left[m \ln\left(\frac{\tau}{\tau_{FK}}\right)\right]\cos\left(\frac{\pi m}{2}\right)}{\sinh^2\left[m \ln\left(\frac{\tau}{\tau_{FK}}\right)\right] + \cos^2\left(\frac{\pi m}{2}\right)} \tag{10}$$

The variables a, b, and m in the above equations lie in the range 0−1, the upper bound being $a = b = m = 1$, which corresponds to Debye-type relaxations.

Deconvolution of the α, β, and γ processes of P3MM was carried out using eqs 6 and 10. The deconvolution was not possible for P3FM and P3CM if the long times peak is considered to be a simple α relaxation. This fact together with the presence of three absorptions detected in the spectra by thermally simulated depolarization techniques led us to consider the long times peak of P3FM and P3CM as a result of the overlapping of the β and α relaxations. The deconvolution of the shortest retardation times absorption or γ peak in the spectra of these polymers was made by mirroring the points with respect to the lines $\tau = \tau_{max}$. Subtracting the symmetric γ peak from the spectra, we proceeded with the deconvolution of the combined α and β peaks by means of eqs 6 and 10. As an example, the overall spectrum and the deconvoluted α, β, and γ peaks for P3CM at 313 K are shown in Figure 5. Therefore, the long times peak for P3FM and P3CM is in fact an αβ absorption.

The accuracy of the spectra was checked by recalculating the loss isotherms from the spectra, and the maximum relative error involved in the calculations was less than 4% in the most unfavorable cases, that is, at frequencies where the dielectric loss measured with different instruments meet and also at the two extremes of the isotherms. As an example, the values at 313 K of the dielectric loss recalculated from the spectra are shown for P3CM in Figure 6. In the inset the relative error in the frequency window 10^{-1}−10^{9} Hz is also shown.

As expected, the narrowness of the α, β, and γ peaks increases with temperature as the retardation spectra of P3CM corresponding to these individual processes indicate (Figure 7). The temperature dependence of the shape parameters describing the deconvoluted peaks for the three polymers is shown in Figure 8. In general, the parameters b and m increase with increasing temperature, leveling off in the high-temperature region, while the values of the parameter a do not follow a definite trend.

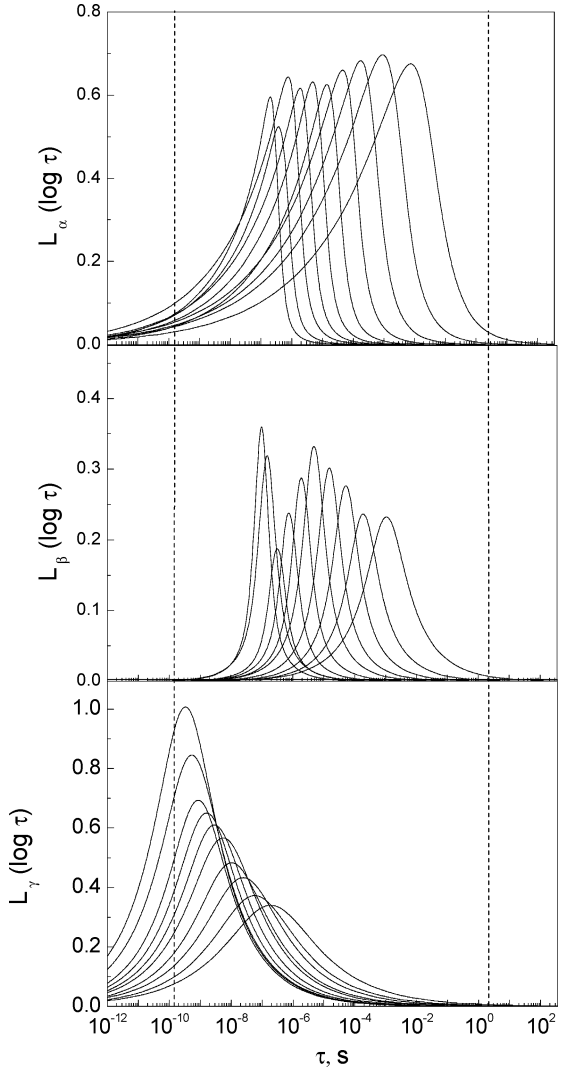

Figure 7. Retardation spectra for the α, β, and γ relaxations of poly(3-chlorobenzyl methacrylate) in the temperature range of 313−413 K at 20 K steps.

The strengths of the relaxations were calculated from the retardation spectra by means of the following expression

$$\epsilon_{r,k} - \epsilon_{u,k} = \int_{-\infty}^{\infty} L_k(\ln \tau)\, d \ln \tau \tag{11}$$

where subscript k refers the type of relaxation (α, β, γ, ...). The pertinent values of $\Delta\epsilon = \epsilon_r - \epsilon_u$, represented as a function of temperature in Figure 9, show that the strength of the α relaxation decreases with increasing temperature. The strengths of the β and γ relaxations of P3MM and P3FM show a weak dependence on temperature, a behavior not shared by the strength of the γ relaxation of P3CM that undergoes a significant increase with temperature.

The Decay Function and the Williams Ansatz. The dielectric permittivity can be written in terms of the normalized buildup function, $\varphi(t)$, as

$$\epsilon(t) = \epsilon_u + (\epsilon_r - \epsilon_u)\varphi(t) \tag{12}$$

where $\varphi(t) = 0$ for $t = 0$ and $\varphi(t) = 1$ for $t \to \infty$. An alternative way of writing eq 12 is[9,11]

$$\epsilon(t) = \epsilon_u + (\epsilon_r - \epsilon_u)\int_{-\infty}^{\infty} L_n(\ln \tau)(1 - e^{-t/\tau})\, d \ln \tau \tag{13}$$

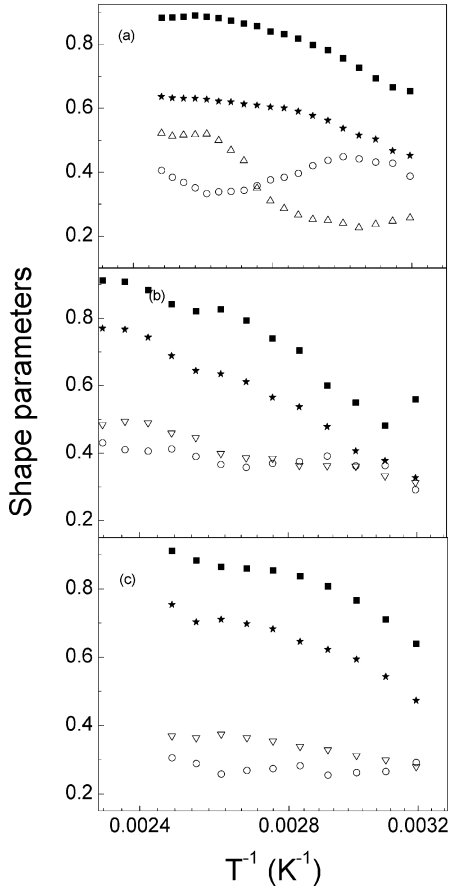

Figure 8. Variation with temperature of the shape parameters of the empirical equations describing the relaxations of poly(3-methylbenzyl methacrylate) (top), poly(3-fluorobenzyl methacrylate) (middle), poly-(3-chlorobenzyl methacrylate) (bottom). Full squares and open circles correspond respectively to the parameters *a* and *b* of the H−N equation, whereas full stars and open triangles represent the parameter *m* of the FK equation for the β and γ relaxations, respectively.

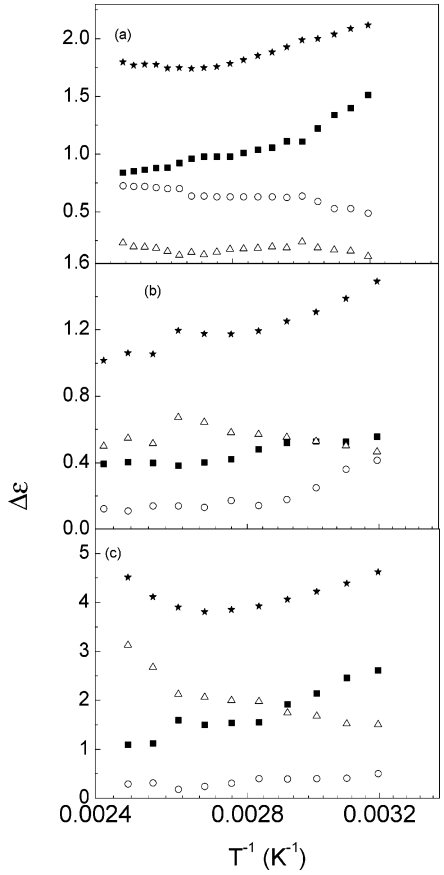

Figure 9. Temperature dependence of the strengths of the α (full square), β (open circles), and γ (open triangles) relaxations for poly-(3-methylbenzyl methacrylate) (top), poly(3-fluorobenzyl methacrylate) (middle), and poly(3-chlorobenzyl methacrylate) (bottom). Full stars represent the total dielectric strength.

where L_n is the normalized retardation spectrum. Taking into account that

$$\phi(t) = 1 - \varphi(t) \tag{14}$$

where $\phi(t)$ is the normalized time dipole autocorrelation function or decay function, eqs 12−14 lead to

$$\phi(t) = \int_{-\infty}^{\infty} L_n(\ln \tau) e^{-t/\tau} \, d \ln \tau = \frac{\int_{-\infty}^{\infty} L(\ln \tau) e^{-t/\tau} \, d \ln \tau}{\int_{-\infty}^{\infty} L(\ln \tau) \, d \ln \tau} \tag{15}$$

The decay functions for P3MM, P3CM, and P3FM calculated from the spectra by means of eq 15 are represented in Figure 10. Williams[1,10,30] assumes the β relaxation arising from restricted motions in a range of local environments, which permit a partial relaxation that leads to an initial drop in $\phi(t)$. When the α relaxation mechanisms are able to cause fluctuations of local environments that lead to the total randomization of the dipoles, $\phi(t)$ becomes zero. Whenever the γ relaxation is well separated from the β absorption, as occurs for P3MM, P3CM, and P3FM, Williams's assumption can be written as

$$\phi(t) = \phi_\alpha(t)[f_\alpha + f_\beta \phi_\beta(t)] + f_\gamma \phi_\gamma(t) \tag{16}$$

where $\phi_\alpha(t)$ and $\phi_\beta(t)$ and $\phi_\gamma(t)$ are the normalized correlation functions calculated by means of eq 15 using the retardation spectra associated respectively with the α and β relaxations. The parameter f_α is the fraction of polarization relaxing through the α process alone, f_β is the fraction of polarization relaxing through the β absorption via de α relaxation, and $f_\gamma = 1 - f_\alpha - f_\beta$ represents the fraction of polarization relaxing via the γ process. Equation 16 is known as the Williams−Watts (WW) ansatz. When the α, β, and γ processes are well separated, the relaxation of the α process is not important until the total relaxation of the secondary absorptions is not complete; i.e., $\phi_\alpha(t) \approx 1$ when $\phi_\beta(t) \approx 0$ and $\phi_\gamma(t) \approx 0$. In this situation, eq 16 becomes

$$\phi(t) = f_\alpha \phi_\alpha(t) + f_\beta \phi_\beta(t) + f_\gamma \phi_\gamma(t) \tag{17}$$

Equation 16 can be written in the frequency domain as

$$\phi^*(\omega) = \frac{\epsilon^*(\omega) - \epsilon_u}{\epsilon_r - \epsilon_u} = L_{i\omega}\left(-\frac{d\phi(t)}{dt}\right) = f_\alpha \phi^*{}_\alpha(\omega) + f_\beta \phi^*{}_\alpha(\omega) \phi^*{}_\beta(\omega) + f_\gamma \phi^*{}_\gamma(\omega) \tag{18}$$

where $L_{i\omega}$ is the Laplace operator and $\phi_k^*(\omega) = L_{i\omega}(-d\phi_k/dt)$, the subscript k meaning α, β, and γ. Illustrative plots showing the dielectric loss calculated from eq 18 for P3CM at 333 K are presented in Figure 11. In general, the dielectric loss obtained from the William ansatz fits rather well to the experimental results.

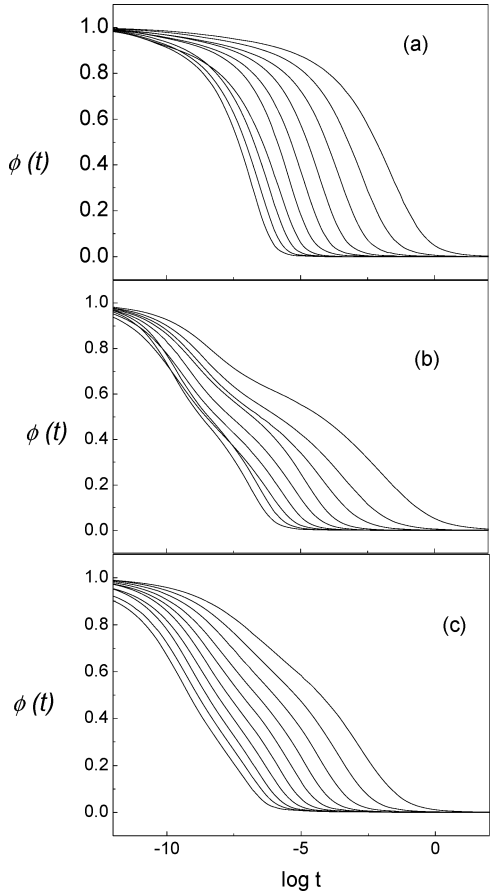

Figure 10. Total decay function for the relaxations of poly(3-methylbenzyl methacrylate) (top), poly(3-fluorobenzyl methacrylate) (middle), and poly(3-chlorobenzyl methacrylate) in the temperature ranges 313−403, 333−423, and 313−403 K, respectively, at 10 K steps.

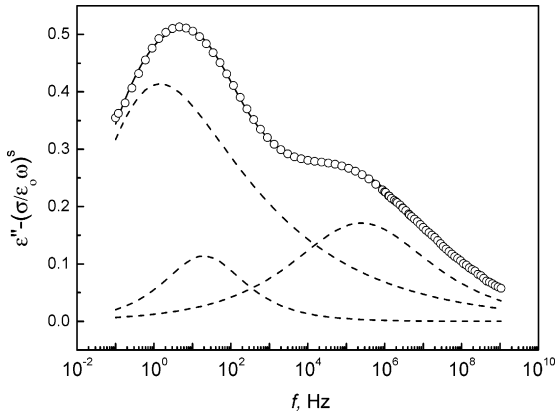

Figure 11. Values of the dipolar dielectric loss at 333 K for poly(3-chlorobenzyl methacrylate): circles and continuous line represent respectively experimental data and experimental results calculated using the Williams−Watts ansatz (eq 18): Dashed curves represent the contributions of the α, β, and γ relaxations.

In the frequency domain, the extended ansatz is given by

$$\phi^*(\omega) = L_{i\omega}\left(-\frac{\mathrm{d}\phi(t)}{\mathrm{d}t}\right) = f_\alpha \phi^*_\alpha(\omega) + f_\beta \phi^*_\beta(\omega) + f_\gamma \phi^*_\gamma(\omega) \tag{19}$$

The temperature dependences of the values of f_α, f_β, and f_γ obtained for P3CM using eqs 18 and 19 are shown in Figure 12. As usual, f_α decreases with increasing temperature whereas f_γ clearly increases. However, f_β does not follow a definite trend. The values of f_α and f_γ obtained by the two methods agree very satisfactorily, but the agreement is not so satisfactory in the case of the β process presumably as a consequence of the errors involved in the determination of the contribution of this weak process to the total relaxation.

Temperature Dependence of the Relaxation Processes. Arrhenius plots for the α, β, and γ relaxations of P3MM, P3CM, and P3FM are shown in Figure 13. The secondary relaxations obey Arrhenius behavior with activation energies of 128 ± 1 and 80 ± 4 kJ/mol respectively for the β and γ relaxations of P3MM. The values of these parameters for P3FM are 112 ± 2 and 49 ± 2 kJ/mol, respectively, and 115 ± 3 and 77 ± 2 kJ/mol for P3CM, respectively. As usual, the dynamic α absorption is described by the Vogel−Fulcher−Tammann−Hesse (VFTH) equation[21]

$$f_{\max} = f_0 \exp\left(-\frac{m}{T - T_V}\right) \tag{20}$$

where f_0 is a prefactor of the order of $(\mathrm{ps})^{-1}$, $f_{\max}$ is the frequency at the peak maximum, and T_V is the so-called Vogel temperature whose value lies in the vicinity of the Kauzmann temperature, that is, the temperature at which the crystal and the glass of the supercooled liquid have the same entropy.[4] The values of m fitting eq 20 to the experimental results are 1990 ± 60, 1350 ± 210, and 1720 ± 130 K respectively for P3MM, P3FM, and P3CM, whereas the values of T_V are 229 ± 2, 256 ± 7, and 230 ± 4 K. Departure of the α process from Arrhenius behavior is defined by the fragility factor $D = m/T_V$ that controls how closely a system obeys the Arrhenius law.[7] The value $D = 10$ is the borderline that separates fragile ($D < 10$) from strong ($D > 10$) glasses.[31] The values of D obtained for P3MM, P3FM, and P3CM are 8.7, 5.3, and 7.5. It should be pointed out that the fragile factors obtained for P3MM and P3CM are near to the upper bound limit of fragile systems.

The ionic conductance follows Arrhenius behavior as the plots of Figure 14 show. The values of the activation energies obtained from the slopes of the plots amount to 100 ± 1, 87 ± 3, and 108 ± 2 kJ/mol respectively for P3MM, P3FM, and P3CM. Therefore, ionic transport in these polymers overcomes energy barriers of the order of those involved in the β process.

By comparing eq 20 with the Doolittle equation,[32] $f_{\max} = f_0 \exp(-B/\Phi)$, where Φ is the relative free volume and B is a parameter close to 1; the relative free volume at T_g is given by

$$\frac{\Phi_g}{B} = \frac{T_g - T_V}{m} \tag{21}$$

The values of Φ_g/B for P3MM, P3CM, and P3FM calculated by this procedure are 0.039, 0.046, and 0.038, respectively, well above the average result of 0.025 ± 0.005 obtained for most polymers.[33] Since B is related to v^*/v_m,[34] where v^* and v_m are respectively the critical volume necessary for a relaxation to take place and the volume of the segments intervening in the relaxation, the high volume of Φ_g/B suggests that $v^* < v_m$ if the iso-free-volume theory holds.

Discussion

The side chains of poly(*n*-alkyl methacrylate)s have a dipole moment associated with the $C(CH_3)C(O)-OCH_2$ ester group of 1.70 D, the direction of which makes an angle of 57° with the $C(CH_3)-C(O)-O$ bond.[35,36] One would expect that most of the polarization relaxes through the β relaxation and the smaller part through the main-chain dynamics reflected in the α relaxation. This holds in poly(methyl methacrylate) (PMM) whose relaxation spectrum exhibits a strong β relaxation and a

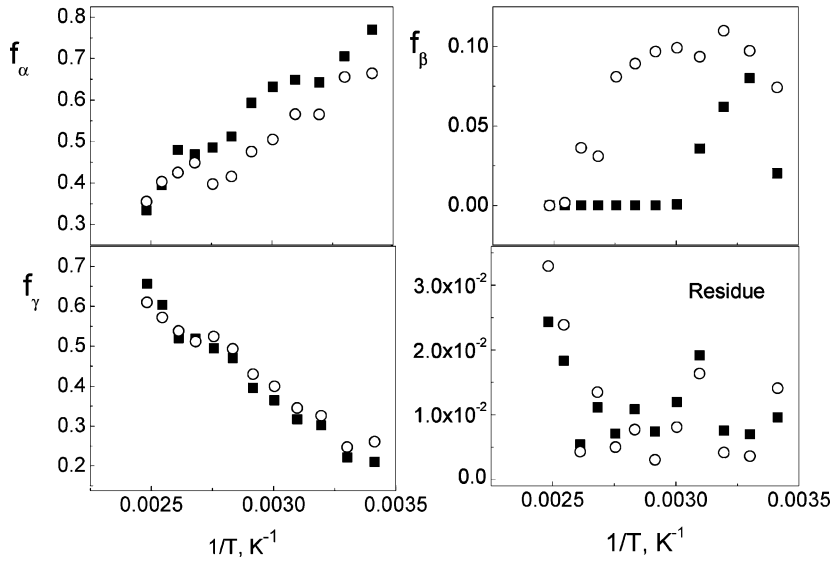

Figure 12. Temperature dependence of the parameters f_α, f_β, and f_γ for poly(3-chlorobenzyl methacrylate) and the mean square error. Open and filled symbols correspond respectively to the Williams ansatz and the extended ansatz.

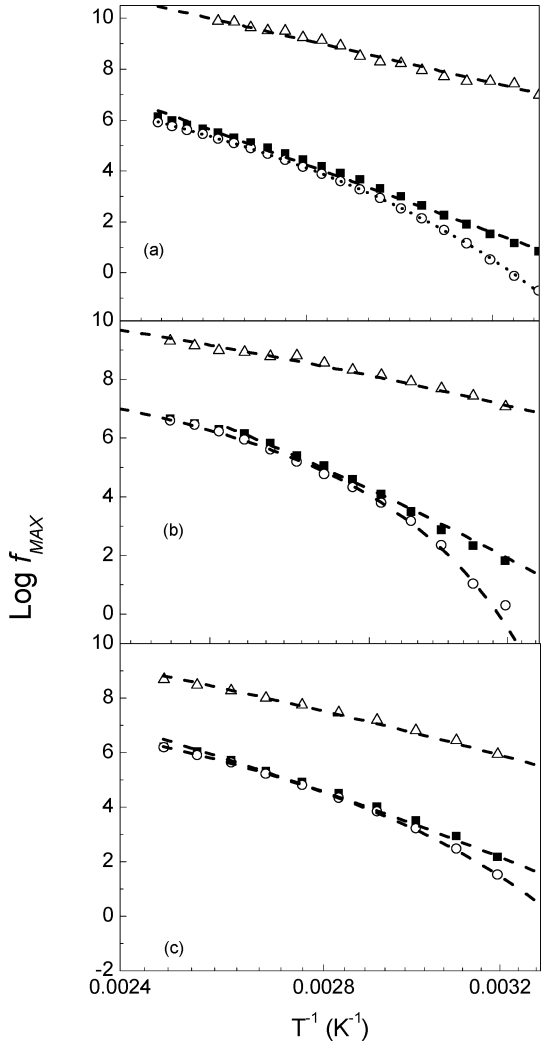

Figure 13. Arrhenius plots for the α (open circles), β (filled squares), and γ (open triangles) relaxations of poly(3-methylbenzyl methacrylate) (top), poly(3-fluorobenzyl methacrylate) (middle), and poly(3-chlorobenzyl methacrylate).

rather weak α relaxation. The relaxation of the polarization through the α process becomes more important as the length of the alkyl residue in the side chain increases. Since the

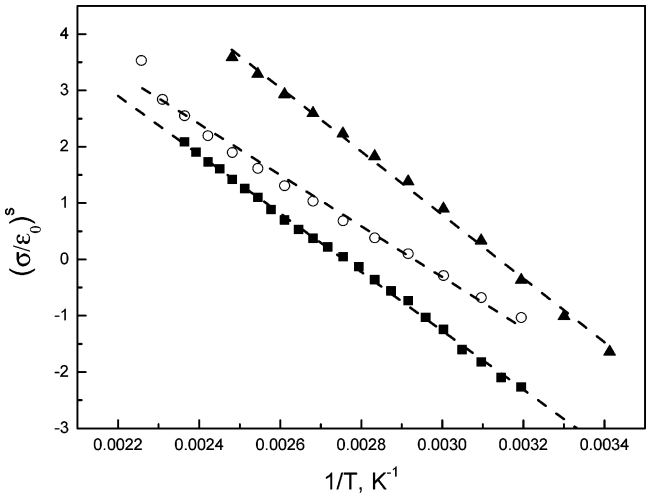

Figure 14. Arrhenius plot showing the temperature dependence of the ionic conductivity, in S/m, of poly(3-methylbenzyl methacrylate) (filled squares), poly(3-fluorobenzyl methacrylate) (open circles), and poly(3-chlorobenzyl methacrylate) (filled triangles).

C(O)−O bond is restricted to the trans state,[37,38] secondary relaxations in the polymers used in this study may not uniquely arise from motions about $C(CH_3)-C(O)O$ bonds but also from motion about $O-CH_2$ bonds and/or CH_2-C^{ar} bonds, where C^{ar} means a carbon of the phenyl group.

The dipole moments corresponding to $C^{ar}-Cl$, $C^{ar}-F$, and $C^{ar}-CH_3$ are respectively 1.55, 1.43, and 0.3 D, and their directions lie along the bonds.[39] The bond lengths of $C^{ar}-F$, $C^{ar}-Cl$, and $C^{ar}-CH_3$ amount to 1.39, 1.77, and 1.53 Å, respectively.[40] Since the $l_{C^{ar}-Cl}$ bond length is significantly lower than the $l_{C^{ar}-F}$, F...C(O) interactions must be lower than Cl...OC(O) interactions. Hence, the $C^{ar}-CH_2$ bond of P3FM surely rotates more freely than that of P3CM. On the other hand, as a consequence of the fact that CH_2-C^{ar} bonds have low barrier energies, the γ relaxation presumably arises from rotations about $C^{ar}-CH_2$ bonds in the polymers investigated. The comparatively low value of the $C^{ar}-F$ bond length favors the free rotation about $C^{ar}-CH_2$ bonds, and as a result, the relaxation strength of the γ relaxation of P3FM must be nearly independent of temperature, as is experimentally found. The significant increase of the strength of the γ process of P3CM with temperature suggests that an increase in temperature

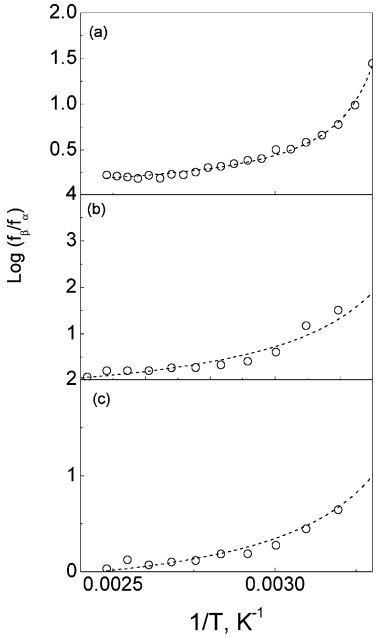

Figure 15. Distance between the maxima of the β and α peaks, expressed as $\log(f_{max;\beta}/f_{max;\alpha})$, for poly(3-methylbenzyl methacrylate) (circles), poly(3-fluorobenzyl methacrylate), and poly(3-chlorobenzyl methacrylate) (squares).

progressively favors the alignment of the dipoles in parallel direction of the ester group and the $C^{ar}-Cl$ bond.

At first sight, the strong overlapping of the α and β relaxations, even at low temperatures, suggests a high complexity in the mechanisms involved in the latter absorption. Despite that, the fact that the activation energies associated with the β relaxations of P3FM, P3CM, and P3MM are similar to those exhibited by poly(*n*-alkyl methacrylate)s suggests that motions about $CH_2-C(O)$ bonds are mainly responsible for the β absorption. The correlations between the dipoles associated with the substituted phenyl moieties and the ester groups, which in turn depend on conformational transitions about $-C(CH_3-C(O)-O-CH_2\,C_6H_5X$ bonds, are responsible for the differences observed on the strengths of the β processes of these polymers.

The distance between the maxima of the deconvoluted α and β peaks, expressed in terms of $\Delta_{\beta-\alpha} = \log(f_{max,\beta}/f_{max,\alpha})$, is plotted as a function of temperature for each polymer in Figure 15. As usual, $\Delta_{\beta-\alpha}$ decreases with increasing temperature until the distance eventually vanishes at about 400 K. The temperature dependence of $\Delta_{\beta-\alpha}$ is described by a Vogel-type equation with the value of T_V close to the glass transition temperature. In fact, the values of T_V for P3MM, P3CM, and P3FM amount to 288, 271, and 246 K, respectively. The temperature dependence of the distance between the peak maxima of the α and γ relaxations Δ' ($= \log(f_{max};\gamma/f_{max};\alpha)$) also obeys Vogel-type equations in the temperature range 303−403 K, as shown in Figure 16. The values of for T_V amount to 277, 216, and 207 K for P3MM, P3CM, and P3FM, respectively. In the splitting region, Δ' remains constant for P3CM and P3FM as a consequence of the similarity of the activation energy of both the γ and α processes in this zone.

Both the Williams ansatz (eq 18) and the extended ansatz (eq 19) give a good account of the relaxation behavior of the polymers. The mean-square errors involved in the evaluation of the dielectric loss at each temperature, named residue in Figure 12, are lower than 6×10^{-3}, 2.5×10^{-3}, and 2.0×10^{-3} for P3FM, P3MM, and P3CM, respectively, even in the most unfavorable cases.

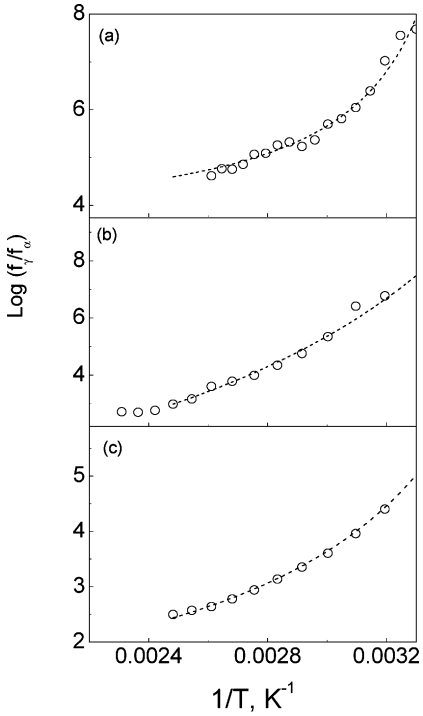

Figure 16. Distance between the maxima of the γ and α peaks, expressed as $\log(f_{max;\gamma}/f_{max;\alpha})$, for poly(3-methylbenzyl methacrylate) (filled squares), poly(3-fluorobenzyl methacrylate) (filled triangles), and poly(3-chlorobenzyl methacrylate) (open circles).

The temperature dependence of the α relaxation is one of the most significant results in this study. Figure 13 shows that the β and γ relaxations obey Arrhenius behavior, but the mechanisms involved in the former process have an activation energy of the same order as that found for the β absorption in poly(*n*-alkyl methacylate)s. Since the $-C(CH_3-C(O)-O-CH_2-$ moiety is common for poly(*n*-alkyl methacrylate)s and poly(benzyl methacrylate)s, the similarity of the activation energy led us to think that the β process arises from motions about the bonds of this moiety as suggested before. However, a new scenario appears in the splitting region earlier postulated but not found in polymers.[3] It refers to the fact that the temperature dependences of the α and β processes not only have the same activation energy in the splitting region but also the prefactors of the exponential term in the Arrhenius equation are similar for both processes. This behavior suggests a profound interdependence between the α and β processes in these polymers.

The normalized dynamic α relaxation in the time domain is inevitably described by the KWW stretch exponential equation[1,3]

$$\phi(t) = \exp\left[-\left(\frac{t}{\tau^*}\right)^{\beta_{KWW}}\right] \tag{22}$$

where β_{KWW} lies in the range $0 < \beta_{KWW} \leq 1$. The temperature dependence of the stretch exponent for P3MM, P3CM, and P3FM is shown in Figure 17. It can be seen that $\beta_{KWW} \approx 0.2$ in the vicinity of T_g and then moderately increases with temperature, reaching a value of about 0.5 at high temperature. The small values of β_{KWW} at low temperatures indicate a rather wide distribution of relaxation times for the α relaxation of the three polymers, which presumably arises from a pronounced dynamic heterogeneity, a feature displayed by other systems. One would expect that due to the fast thermal fluctuations, each relaxing entity would see the same environment at high temperatures, leading to a Debye relaxation.[31] However, this

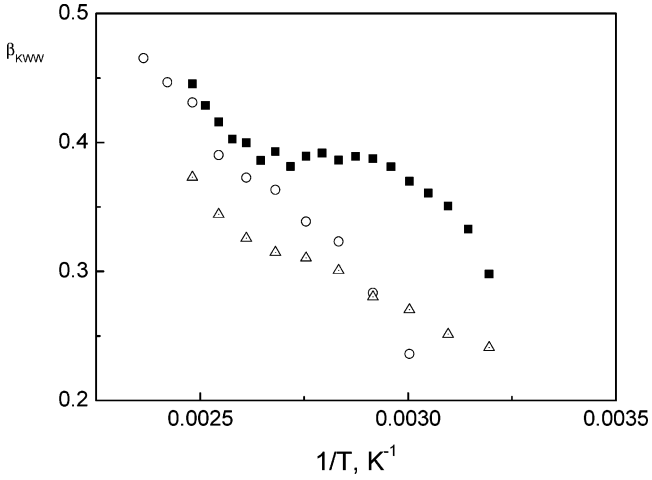

Figure 17. KWW stretch exponent for poly(3-methylbenzyl methacrylate) (filled squares), poly(3-fluorobenzyl methacrylate) (open circles), and poly(3-chlorobenzyl methacrylate) (open triangles).

and other dielectric results do not show a stretch exponent independent of temperature in the splitting region.

Conclusions

Whereas for most polymers the α and β absorptions merge together forming the $\alpha\beta$ relaxation at temperatures well above T_g, the merging of these relaxations for the halogenated poly(benzyl methacrylate)s studied in this work already occurs at temperatures slightly higher than the glass transition temperature.

The onset detected in the α relaxation of poly(*n*-alkyl methacrylate)s and other polymers like poly(5-acryloxy-5-methyl-1,3-dioxacyclohexane) is absent in the polymers studied in this work.

A new scenario, already suggested but still not found, appears in the temperature dependence of the relaxations of these polymers. This scenario is connected with the fact that the curves describing the variation of the relaxation times of the α and β absorptions with temperature are nearly similar for both processes at high temperature. This behavior suggests a profound interdependence between the α and β processes in these polymers.

Theories quantitatively explaining the big influence of the fine chemical structure on high-frequency chain dynamics are still lacking.

Acknowledgment. This work was financially supported by the DGCYT and CAM through Grants MAT2002-04042-C02, MAT2005-05648-C02-02, and GR/MAT/0723/2004. L.G. and D.R. thank the FONDECYT for partial financial support through Grants 21050956 and 1050962, respectively.

References and Notes

(1) Williams, G. In *Keynote Lectures in Selected Topics of Polymer Science*; Riande, E., Ed.; CSIC: Madrid, 1995; Chapter 1.
(2) Stillinger, F. K. *Science* **1995**, *262*, 1935.
(3) Garwe, F.; Schönhals, A.; Lockwenz, H.; Beiner, M.; Schröter, K.; Donth, E. *Macromolecules* **1996**, *29*, 247.
(4) Ediger, M. D.; Angell, C. A.; Nagell, S. R. *J. Phys. Chem.* **1996**, *100*, 13200.
(5) Götze, W.; Sjögren, L. *Transp. Theory Stat. Phys.* **1995**, *24*, 801.
(6) Götze, W.; Sjögren, L. *Rep. Prog. Phys.* **1992**, *55*, 241.
(7) Angell, C. A. In *Complex Behavior of Glassy Systems*; Proceedings of the XIV Sitges Conference, Sitges, Barcelona, Spain, 10−14 June 1996; Rubí, M., Pérez-Vicente, C., Eds.; Springer-Verlag: Berlin, 1997.
(8) Angell, C. A. *Science* **1995**, *262*, 1924.
(9) Williams, G. *Trans. Faraday Soc.* **1964**, *62*, 2091.
(10) Williams, G. *Adv. Polym. Sci.* **1979**, *33*, 60.
(11) McCrum, N. G.; Read, B. E.; Williams, G. *Anelastic and Dielectric Effects in Polymeric Solids*; Wiley: New York, 1967; Chapter 4; Dover: Mineola, NY, 1991.
(12) Schönhals, A. In *Broadband Dielectric Spectroscopy*; Springer-Verlag: Berlin, 2003; Chapter 7.
(13) Riande, E.; Díaz-Calleja, R. *Electrical Properties of Polymers*; Marcel Dekker: New York, 2004; Chapter 8.
(14) Bergman, R.; Alvarez, F.; Alegría, A.; Colmenero, J. *J. Chem. Phys.* **1998**, *109*, 7546.
(15) Gómez, D.; Alegría, A.; Arbe, A.; Colmenero, J. *Macromolecules* **2001**, *34*, 503.
(16) Schröter, K.; Unger, R.; Reissig, S.; Garwe, F.; Kahle, S.; Beiner, M.; Donth, E. *Macromolecules* **1998**, *31*, 8966.
(17) Kahle, S.; Korus, J.; Hempel, R.; Unger, R.; Höring, S.; Schröter, K.; Donth, E. *Macromolecules* **1997**, *30*, 7214.
(18) Casalini, R.; Fioretto, D.; Livi, A.; Luchéis, M.; Rolla, P. A. *Phys. Rev. B* **1997**, *56*, 3016.
(19) Huang, Y.-N.; Saiz, E.; Ezquerra, T.; Guzmán, J.; Riande, E. *Macromolecules* **2002**, *35*, 2926.
(20) Álvarez, C.; Lorenzo, V.; Riande, E. *J. Chem. Phys.* **2005**, *122*, 194905.
(21) Vogel, H. *Z. Phys.* **1923**, *22*, 645. Fulcher, J. S. *J. Am. Ceram. Soc.* **1925**, *8*, 839. Tammann, G.; Hesse, W. Z. *Anorg. Allg. Chem.* **1926**, *156*, 245.
(22) Dominguez-Espinosa, G.; Díaz-Calleja, R.; Riande, E.; Gargallo, L.; Radic, D. *J. Chem. Phys.* **2005**, *123*, 114904.
(23) Press, W. H.; Teukolsky, S. A.; Vetterling, W. T.; Flannerty, B. P. In *The Art of Scientific Computing*, 2nd ed.; Cambridge University Press: New York, 1992; Chapter 18.
(24) Morozov, V. A *Methods for Solving Incorrectly Posed Problems*; Springer: New York, 1984.
(25) Provencher, S. W. *Comput. Phys. Commun.* **1982**, *27*, 229.
(26) Havriliak Jr., S.; Havriliak, S. J. *Dielectric and Mechanical Relaxation in Materials*; Hanser: New York, 1997; Chapter 1.
(27) Reiner Zorn, A. *J. Polym. Sci., Part B: Polym. Phys.* **1999**, *37*, 1043.
(28) Fuoss, R.; Kirkwood, J. G. *J. Am. Chem. Soc.* **1941**, *63*, 385.
(29) Macdonald, J. R. *Impedance Spectroscopy*; Wiley-Interscience: New York, 1987; p 41.
(30) Williams, G. In *Comprehensive Polymer Science*; Allen, G., Bevington, J. C., Eds.; Pergamom: Oxford, 1989; Vol. 2, Chapter 7, p 601.
(31) Lunkenheimer, P.; Schneider, U.; Brand, R.; Loidl, A. *Contemp. Phys.* **2000**, *41*, 15.
(32) Doolittle, A. K.; Doolittle, D. B. *J. Appl. Phys.* **1957**, *28*, 901.
(33) Ferry, J. D. *Viscoelastic Properties of Polymers*, 2nd ed.; Interscience: New York, 1970; p 316.
(34) Cohen, M. H.; Turnbull, D. *J. Chem. Phys.* **1959**, *30*, 748.
(35) Saiz, E.; Mark, J. E.; Flory, P. J. *Macromolecules* **1977**, *10*, 967.
(36) Riande, E.; Saiz, E. *Dipole Moments and Birefringence of Polymers*; Prentice Hall: Englewood Cliffs, NJ, 1992.
(37) Flory, P. J. *Configurational Properties of Polymer Chains*; Interscience: New York, 1969.
(38) Mattice, W. L.; Suter, U. W. *Conformational Properties of Large Molecules*; Interscience: New York, 1994.
(39) McClellan, A. L. *Tables of Experimental Dipole Moments*; Rahara Enterprises: El Cerrito, CA, 1974; Vol. 2.
(40) Hopfinger, A. J. *Conformational Properties of Macromolecules*; Academic Press: London, 1973; p 3.

MA052381C